NUMERICAL INVESTIGATION OF THE IN-PLANE BEHAVIOUR OF CONCRETE MASONRY INFILLED RC FRAMES UNDER QUASI-STATIC CYCLIC LOADING

Rahimi, Reza[1] and Liu, Yi[2]

ABSTRACT

This paper presents the development of a nonlinear finite element model using the OpenSEES program to simulate the in-plane response of concrete masonry infilled RC frames subjected to quasi-static cyclic loading. The nonlinear fibre element and shell element were employed to model the RC frame and the infill wall, respectively. The damage mechanics and smeared cracking model was adopted to simulate cracking pattern and failure mode of the infill. The zero-length element was applied to capture the interfacial behaviour between the RC frame and the masonry infill wall. Concurrent with the numerical study, an experimental program was conducted where five infilled RC frames were subjected to in-plane, quasi-static cyclic loading to failure. The infill opening and interfacial gap were implemented as parameters. The results of the experimental study were used to verify the model. It was shown that the model is capable of simulating the nonlinear behaviour of the masonry infilled RC frame and the effect of the interfacial gap and the infill opening were also adequately captured.

KEYWORDS: *masonry infilled wall, quasi-static cyclic loading, nonlinear finite element model, OpenSEES*

INTRODUCTION

Masonry infill walls play an important role in the response of masonry infilled frames subjected to in-plane loading. Previous research ([1-4]) showed that the masonry infills can significantly impact the stiffness, strength, and failure mode of the frame system under static loading. The degree of impact is dependent on the extent of interaction between the infill and the bounding frame. The infill effect on the frame system dynamic behaviour was also studied through experimental tests ([3-5]) as well as finite element simulations ([6], [7]). These studies showed that the infills increased the strength, ductility and energy dissipation of the frame system even

[1] Research Assistant, Department of Civil and Resource Engineering, Dalhousie University, 5248 Morris St., Halifax, NS, Canada, reza.rahimi@dal.ca

[2] Professor and Department Head, Department of Civil and Resource Engineering, Dalhousie University, 5248 Morris St., Halifax, NS, Canada, yi.liu@dal.ca

after extensive cracking. However, due to the complexity of the problem stemming from various types of component materials (frame and infill), the difference in material behaviour and development of inelasticity of both components at high load levels, development of rational and comprehensive design methods remains a challenge. Recent research has increasingly implemented numerical modelling using finite element methods ([8], [9]) as an effective tool to provide results on a wide range of parameters which were often beyond the feasibility of physical tests. These models were mainly encoded using commercial software. Although these studies demonstrated the capability of computer modelling in the simulation of masonry infilled frames, there was commonly a lack of information provided on the input material parameters and analysis procedure, which makes it difficult for others to reproduce the model and associated results.

This paper is motivated to develop a numerical model capable of simulating the dynamic behaviour of masonry infilled RC frames of varying material and geometric properties. The finite element package, OpenSEES, which is available in the public domain is used for the modelling. The model development and its validation against experimental results of masonry infilled RC frames tested under both static and quasi-static cyclic loading are presented in this paper. It is shown that the model is capable of simulating both monotonic and cyclic behaviour of the infilled frame and capturing the strength and stiffness deterioration as well as pinching and softening characteristics of hysteresis curves.

EXPERIMENTAL PROGRAM

Two sets of experiments of concrete masonry infilled RC frames subjected to in-plane loading were conducted in the same research group by Hu [2] and Steeves [5]. While using the same geometry and materials for infilled specimens, one set of experiments were conducted under static loading whereas the other set was conducted under quasi-static loading. For ease of reference, critical information of the experimental program pertinent to the modelling is summarized in the following.

Table 1 summarizes the specimens used in these experimental programs. Six specimens were tested under static loading with interfacial gaps being the main parameter whereas five specimens were tested under quasi-static cyclic loading with both interfacial gaps and infill openings incorporated in the specimen parameter design. Figure 1 shows the dimensions and reinforcement details used for all specimens. The RC frame top beam and columns were 180 mm by 180 mm square sections reinforced with four 10M deformed steel rebars and 10M stirrups spacing at 100 mm center-to-center. The base beam was a 250 mm square section reinforced with four 15M rebars and 10M stirrups spacing at 100 mm center-to-center. Half scale concrete blocks of standard 200 mm CMUs were used in a running bond pattern to construct the masonry infill wall. Two of the infilled specimens with predefined gap also had a window opening accounting for 20% of the infilled area with an aspect ratio of 1:1.5.

Table 1: Summary of the Test Specimens

Static Test		Quasi-Static Test		
Specimen ID	Gap	Specimen ID	Gap	Window Opening/Infill Area Ratio
BF	N.A.	BF	N.A.	N.A.
IF-NG	-	IF-FG12	12 mm Top Gap & 12 mm Side Gap (6 mm each side)	-
IF-TG7	7 mm Top Gap	IF-W-TG12	12 mm Top Gap	20%
IF-TG12	12 mm Top Gap	IF-TG25	25 mm Top Gap	-
IF-SG7	12 mm Side Gap (3.5 mm each side)	IF-W-SG12	12 mm Side Gap (6 mm each side)	20%
IF-SG12	12 mm Side Gap (6 mm each side)	-	-	-

Figure 2(a) shows a schematic view of the test set-up. A hydraulic actuator was used to apply both static and quasi-static lateral load. The base beam of the frame was clamped to the strong floor and braced using hydraulic jacks to prevent potential in-plane movements. Displacement transducers (LVDTs) were used to measure the specimen displacement. In the case of quasi-static loading, two threaded rods running the full length of the frame top beam were installed on the specimens to enable the pulling action on the specimen. During the static test, the lateral load was applied gradually at a rate of 6 kN per minute to the frame top beam until the failure of the specimen. In the cyclic loading protocol, a sequential phased displacement technique was used to apply the displacement to the infilled frame based on the procedure specified by the Applied Technology Council (ATC 24) for cyclic load test [10]. Figure 2(b) shows the lateral quasi-static loading protocol where the peak amplitude for each set of cycles is defined based on the yield deformation. The displacement amplitudes were applied at a rate of 10 mm per minute to ensure the quasi-static nature of the loading.

NUMERICAL MODELING

The OpenSEES [11] is an open-source object-oriented software program developed primarily for simulation of structural seismic behaviour. The robustness and versatility of the program for handling different structural applications as well as its computational efficiency make the OpenSEES a strong competitor to other commercial software such as ANSYS and ABAQUS. The OpenSEES has been successfully used ([12]- [13]) to model different aspects of infilled frames. While previous studies mainly used line elements to simulate the behaviour of infilled frame, this paper adopted nonlinear beam-column elements and continuum elements to model the RC frame

and the infill respectively. The use of these elements enabled the study of softening, cracking and failure mode of the infilled frame in addition to obtaining its load vs. displacement response and ultimate strength.
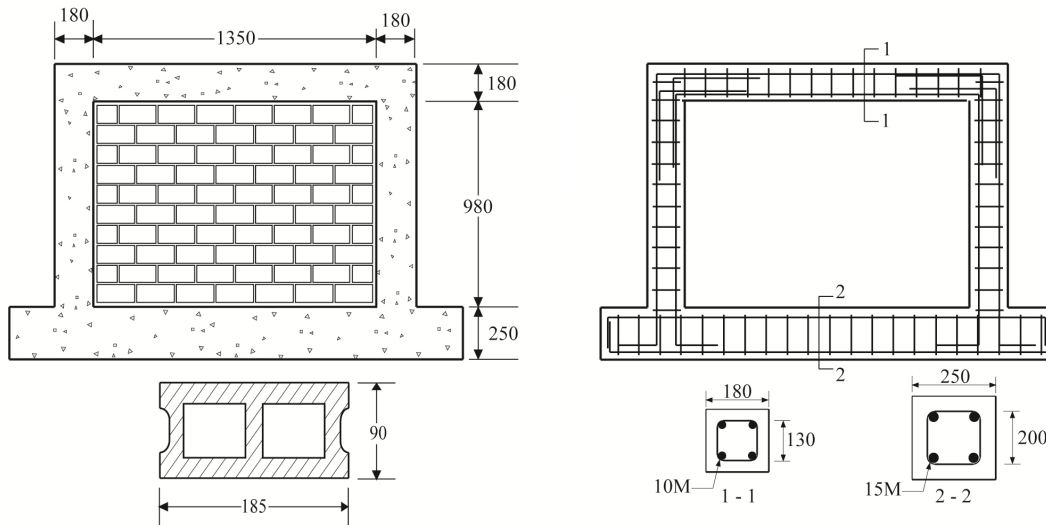

Figure 1: Details of Test Specimens (unit: mm)

(a)

(b)
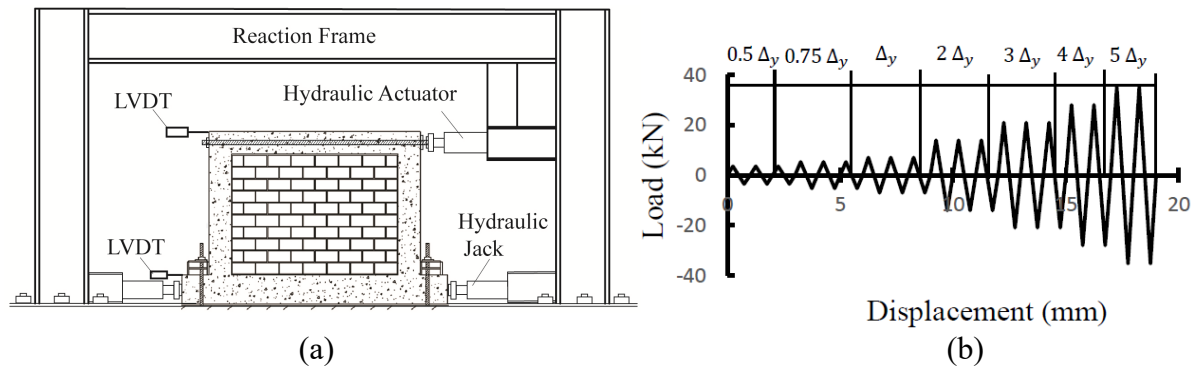
Figure 2: (a) Schematic View of Test Set-Up; (b) Loading Protocol for Quasi-Static Loading

### Modelling of the Bare RC Frame

A fibre element, available in the OpenSEES element library, was employed to model the reinforced concrete frame members. The fibre element is essentially a two-node beam-column element with 6 degrees of freedom at each node. In this case, the reinforced concrete section was divided into three different segments including the concrete cover, concrete core and steel reinforcement. Figure 3, shows both the fibre discretization and the number of fibres (Nf) of each segment used in the model. A convergence study was conducted on the number of the fibres in each segment and the number of fibres chosen was able to provide accurate results with reasonable computational time.
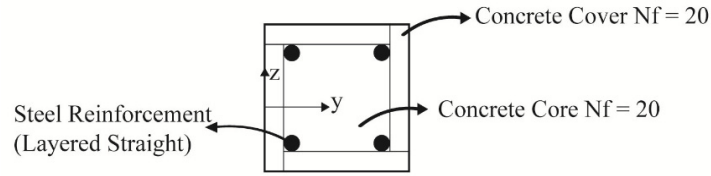
Figure 3: Fibre Discretization of Reinforced Concrete Section

The static stress-strain model developed by Menegotto-Pinto and modified by Filippou et al. [14] was used to model the steel rebar behaviour considering strain hardening in steel. Pinching and softening, observed in the hysteretic load vs. displacement curves of reinforced concrete frames are believed to be associated with concrete cracking and bond-slip effect of steel rebar ([14]). The bond-slip effect refers to a phenomenon where a steel bar, when embedded in concrete, does not show a pronounced yield plateau and the "apparent yield stress" is lower than the yield stress of a bare steel bar. To simulate the bond-slip effect in the proposed model, the reloading and unloading paths in the steel rebar stress-strain relation were adopted from work by Monti and Spacone [15]. Figure 4 (a) shows the complete material constitutive model used for the steel rebar.

The compressive stress-strain envelope for concrete was based on the model proposed by Mander et al. [16]. In the case of the quasi-static cyclic loading, the unloading and reloading responses defined by Karsan-Jirsa [17] were implemented. The falling branch of the stress-strain curve in tension was defined by an exponential curve. Figure 4 (b) presents the stress-strain curve for concrete.


(a)

(b)
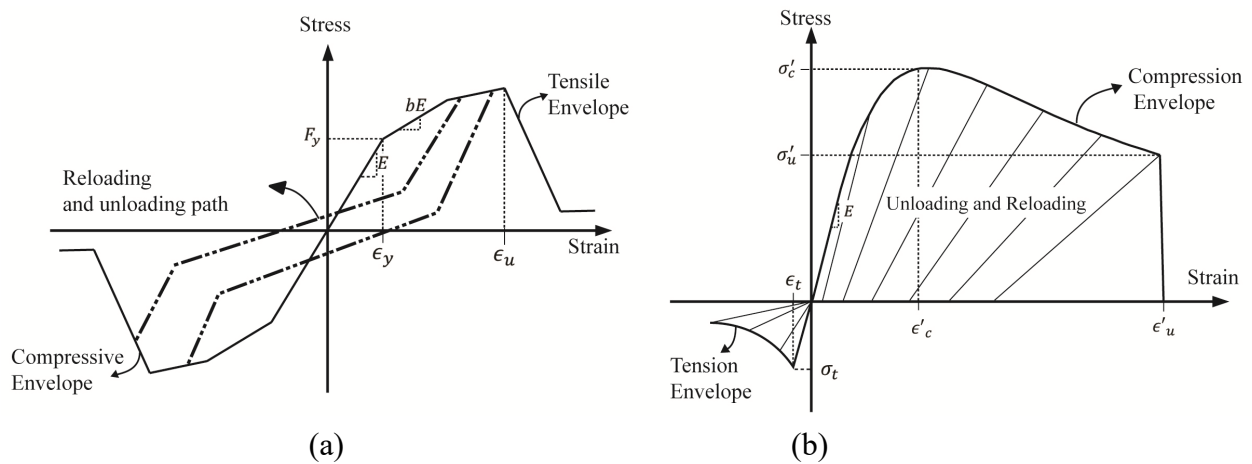
Figure 4: Stress-Strain Curve; (a) Steel Rebar, (b) Concrete

Modelling of the Masonry Infill Wall
The Shell element, ShellMITC4 [18], was used to model the masonry infill wall. To simulate the stress distribution across the thickness of the masonry infill wall, a multi-layer section, developed by Lu et al. [19], was employed. By discretizing each face-shell of the masonry block into multiple fully-bounded layers in the thickness direction, a multi-layered section of the shell element was

used to capture the three-dimensional stress distribution of the masonry infill wall. It was assumed that the stresses in each layer will remain consistent with the stresses at the mid-surface of the same layer [19]. A convergence study was conducted to determine the mesh size and number of layers. Figure 5 shows mesh sizes and number of layers for a single block, used in this study.
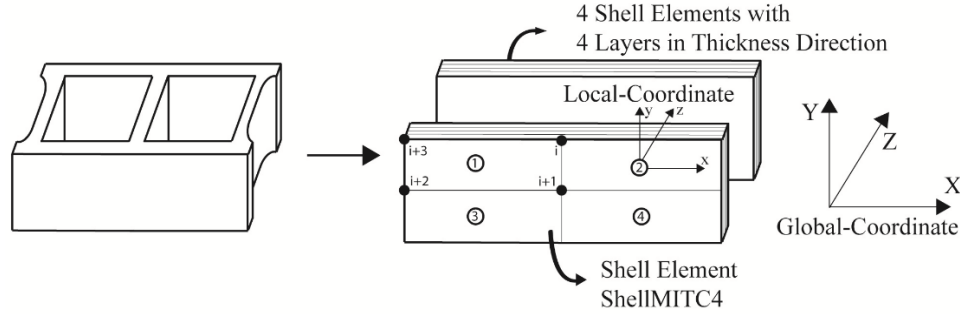

Figure 5: Mesh Size and Number of Layers of Shell Element

The material constitutive model for masonry developed by Lu et al. [19], was employed where both damage mechanics and smeared crack concept were taken into account. Figure 6 (a) and (b) show the constitutive models used for masonry in tension and compression and Eqns (1) and (2) provide the expressions.

$$\sigma'_c = \begin{bmatrix} 1 - d_1 & \\ & 1 - d_2 \end{bmatrix} D_e \epsilon'_c \tag{1}$$

$$\tau = \beta G \gamma \tag{2}$$

where σ'_c and ϵ'_c show stress and strain tensor, respectively; D_e represent the elastic stiffness matrix. The d_1 and d_2 in Eqn (1) are the damage parameters calculated based on the damage evolution curves under tension and compression, respectively. In the shear stress-strain relation expressed in Eqn (2), β represents the shear retention factor which accounts for shear stress deterioration after cracking.
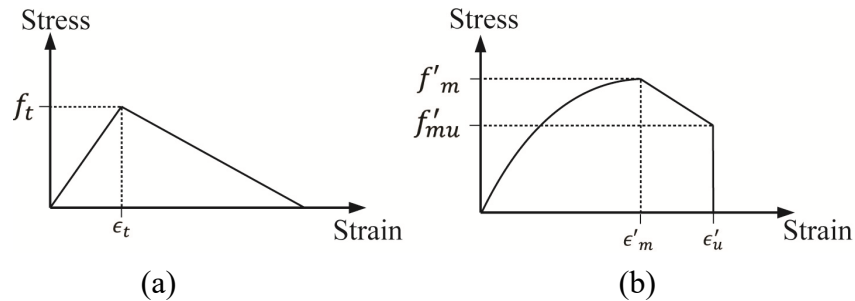
Figure 6: Smeared Crack Constitutive Model; (a) Tensile Behaviour of Orthotropic Model; and (b) Compressive Behaviour of Orthotropic Model

The interface of the concrete frame and masonry infill wall was modelled using the nonlinear zero-length element available in OpenSEES. The zero-length element was placed at each point of

contact between the masonry infill wall and the bounding frame, connecting the fibre element and the shell element. The zero-length element was assumed to be linear elastic with a high stiffness in compression and practically zero stiffness in tension.

MODEL VALIDATION

The model was validated using the lateral load vs. displacement responses in both monotonic and cyclic loading tests for the bare frame as well as masonry infilled frame specimens. Table 2 summarises experimental and FE results on the strength and stiffness of each specimen. The strength is determined as the maximum load obtained from either static or hysteretic response curves, and the stiffness is determined as the secant stiffness connecting the maximum load point and the origin. In both loading cases, the test-to-FE ratios for both strength and stiffness were close to unity. The COV for stiffness test-to-FE ratio is higher of the two but both are less than 15%, which can be considered relatively low from a practical standpoint for masonry. This suggests that the model is capable of providing accurate values for important response indicators of specimens including those with interfacial gaps and infill openings.

Table 2: Summary of the Numerical Results vs. Experimental Data

	Static Test						Quasi-Static Test						
ID	**Strength (kN)**			**Stiffness at Ultimate (kN/mm)**			**ID**	**Strength (kN)**			**Stiffness at Ultimate (Loading Portion) (kN/mm)**		
	F_{exp}	F_{FE}	$\dfrac{F_{exp}}{F_{FE}}$	K_{exp}	K_{FE}	$\dfrac{K_{exp}}{K_{FE}}$		F_{exp}	F_{FE}	$\dfrac{F_{exp}}{F_{FE}}$	K_{exp}	K_{FE}	$\dfrac{K_{exp}}{K_{FE}}$
BF	58.5	59.1	0.99	1.7	1.7	0.99	BF	60.5	59.8	1.01	1.19	1.16	1.02
IF-NG	133.6	134.9	0.99	12.2	10.2	1.20	IF-FG12	79.5	72.1	1.10	2.52	2.65	0.95
IF-TG7	129.0	133.3	0.97	8.4	8.3	1.02	IF-W-TG12	71.8	64.2	1.12	2.68	2.66	1.01
IF-TG12	102.0	109.1	0.93	3.6	3.5	1.04	IF-TG25	74.5	74.3	1.00	5.54	6.80	0.81
IF-SG7	134.0	129.5	1.03	7.9	6.6	1.19	IF-W-SG12	66.9	70.0	0.96	2.13	1.92	1.11
IF-SG12	114.0	119.6	0.95	2.5	3.1	0.85	-	-	-	-	-	-	-
AVG			0.98			1.05	AVG			1.04			0.98
C.O.V (%)			3.6			12.7	C.O.V (%)			6.7			11.1

Bare Frame (BF)

Figure 7 shows both the hysteretic and backbone behaviour of FE versus experimental results in the case of quasi-static cyclic loading. The FE model simulated the hysteric behaviour in terms of loading and unloading paths with a good agreement with the experimental curves. The backbone

curve simulation showed a marked accuracy. This suggests that use of the fibre beam-column element is adequate for modelling bare frames.

(a)   (b)
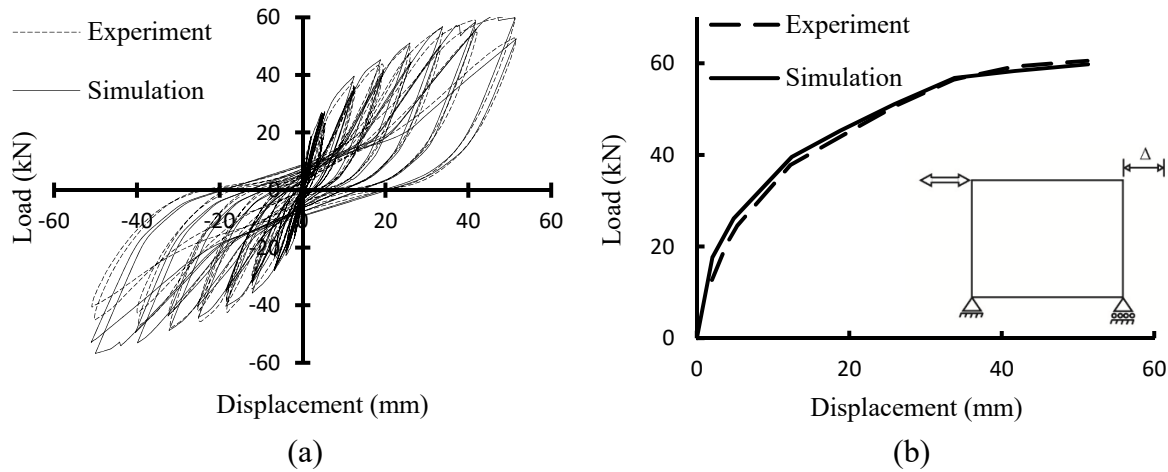
Figure 7: Load vs. Displacement Response of Bare Frame under Quasi-Static Cyclic Loading, (a) Hysteresis Response, (b) Backbone Curve

Masonry Infilled Frames

Figure 8 compare the monotonic load vs. displacement response of the infilled frame. The proposed model simulated accurately the rising branch of the static response of the masonry infilled frame. The difference observed at the post-ultimate portion of curves is believed to be associated with the residual strength of masonry beyond the ultimate strain. In the model, this strength was considered as zero but in the experiment, residual strength in the masonry units was observed after the ultimate load was reached.
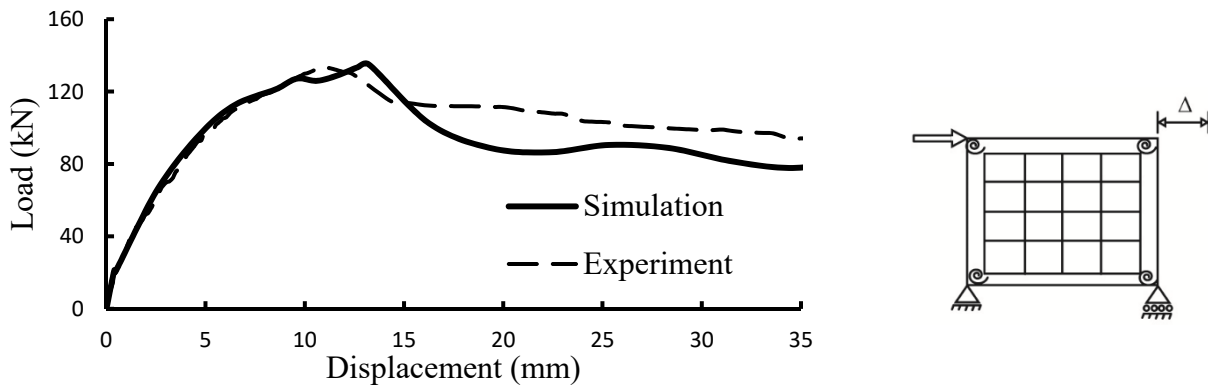

**Figure 8: Load vs. Displacement Behaviour of Masonry Infilled Frame under Monotonic Loading**

Figure 9 compares the hysteretic as well as backbones curves for the specimen IFGT25 (infilled frame with 25 mm top gap) under the quasi-static cyclic loading. Overall, the simulated hysteresis curves compare reasonably well with the experimental results.

The performance of the model is further illustrated in Figure 10(a) and (b) where the loading and unloading stiffness of the specimen in each cycle is compared. The reloading stiffness is defined as the secant stiffness from the origin to the peak load at each cycle. The unloading stiffness was defined as the secant stiffness from the peak load to point of zero loads within the half cycle. The degradation of stiffness as loading progressed is accurately captured.
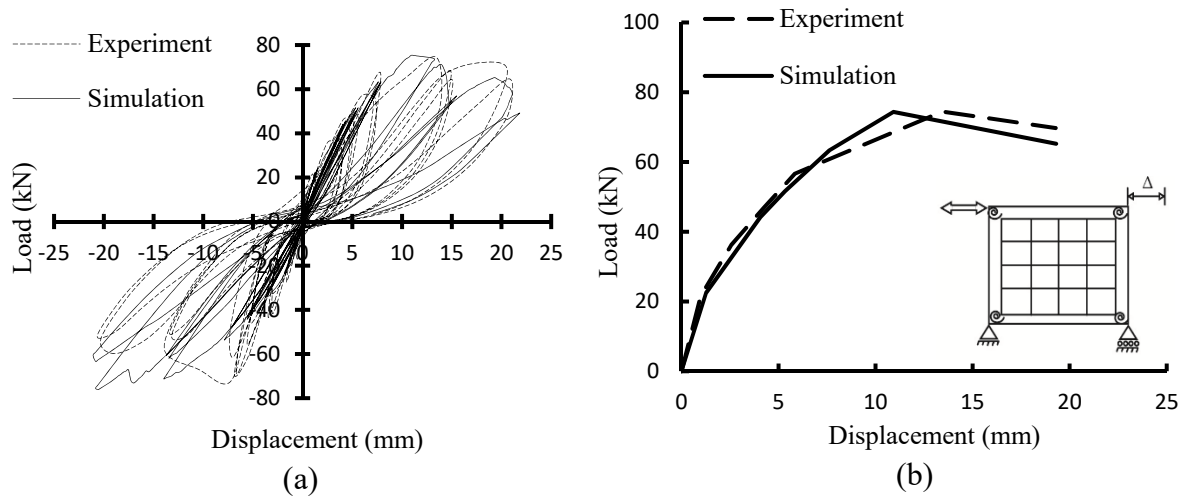

Figure 9: Load vs. Displacement Response of Infilled Frame in Case of Quasi-Static Cyclic Loading; (a) Hysteresis Response, (b) Backbone Curve
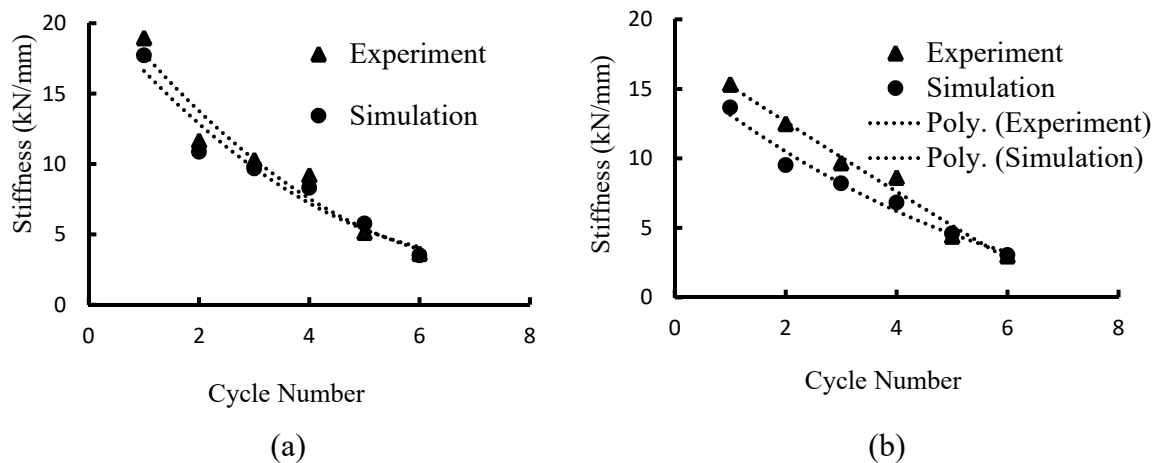
Figure 10: Stiffness vs. Cycle Numbers; (a) Loading Stiffness, (b) Unloading Stiffness

The failure mode of all specimens predicted by the FE model was corner crushing, which agreed with the experimental observation. Figure 11 shows the comparison of failure modes for specimen IFTG25 noting that failure in the FE model (Figure 11 (b)) is indicated through the normal stress contours at the ultimate load. In Figure 11 (b) the maximum normal stress is shown in dark blue colour, coinciding with the corner crushing locations at the top left and bottom right corner of the

infill. The high normal stress forming a strip from the top left corner to the bottom right corner of the infill shown in Figure 11 (b), agreed well with the diagonal cracking pattern observed during the experimental test.

(a)   (b)
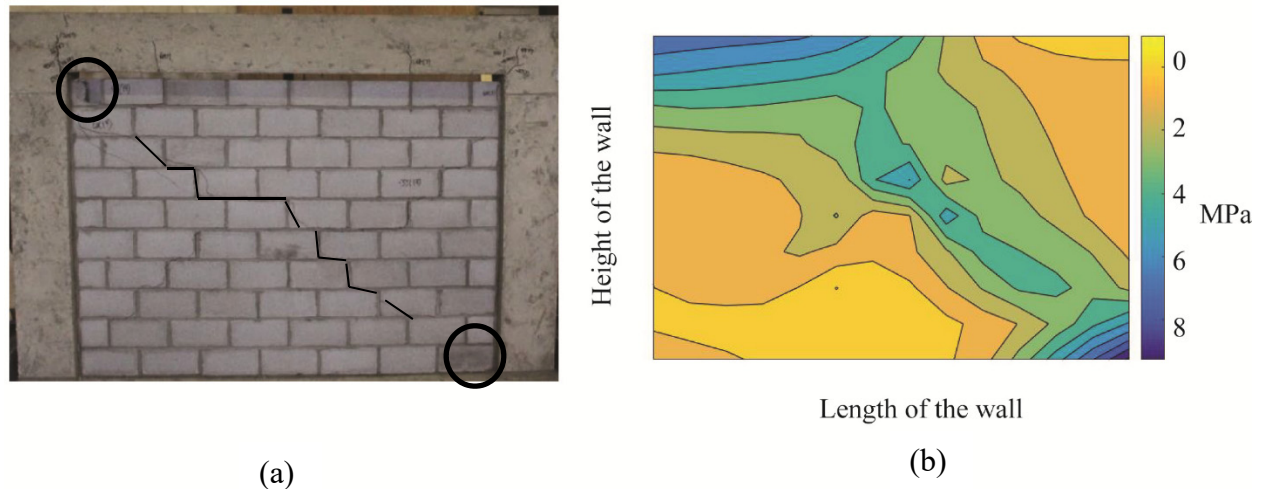
Figure 11: Failure Mode of Specimen IFTG25; (a) Experimental Observation (b) Stress Distribution Contour of Simulated Model

CONCLUSION

A finite element model was developed to simulate the behaviour of concrete masonry infilled RC frames subjected to in-plane lateral loading. The OpenSEEs program was used due to its availability to public and computational efficiency as well as its capability in simulating seismic behaviour. Details of geometric and material models for each component of infilled frame are described in the paper. The model was validated using experimental results for both monotonic and quasi-static cyclic loading. The validation showed that the FE model is capable of simulating the load vs. displacement behaviour and capturing the cracking and failure modes of masonry infilled frames under both loading conditions. In the case of cyclic loading, the hysteretic behaviour with stiffness degradation was accurately simulated. Since the experimental specimens incorporated parameters such as infill openings and interfacial gaps, the successful validation suggests that the developed FE is also capable of reflecting the effect of geometric irregularities in the results. While further validation with test data is still on-going, the results so far are promising. Since it is computationally efficient, it can be an attractive research tool to aid in seismic analysis and design of masonry infilled frames.

ACKNOWLEDGMENTS

REFERENCES

[1] Al-Chaar, G. (2002). "Evaluating strength and stiffness of unreinforced masonry infill structures." *(No. ERDC/CERL-TR-02-1). The U.S. Army Engineer Research and Development Center (ERDC)*, Champaign, Ill.

[2] Hu, C. (2015). "Experimental study of the effect of interfacial gaps on the in-plane behaviour of masonry infilled RC frames." *master's thesis, Dalhousie University*, Halifax, NS, Canada.

[3] Mehrabi, A. B., Benson Shing, P., Schuller, M. P., & Noland, J. L. (1996). Experimental evaluation of masonry-infilled RC frames. *J. of Struct. Eng.*, 122(3), 228-237.

[4] Mosalam, K. M., White, R. N. and Gergely, P. (1997). "Static response of infilled frames using quasi-static experimentation." *J. Struct. Eng.,* 123(11), 1462-1469.

[5] Steeves, R. J. (2017). "Quasi-static testing of masonry infilled RC frames with interfacial gap." *master's thesis, Dalhousie University*, Halifax, NS, Canada.

[6] Shing, P. B. and Mehrabi, A. B. (1997). "Finite element modeling of masonry-infilled RC frames." *J. Struct. Eng.,* 123(5), 604-613.

[7] Chen, X. and Liu, Y. (2015). "A finite element study of the effect of vertical loading on the in-plane." *J. Eng. Struct.,* 85, 226–235.

[8] Stavridis, A. and Shing, P. B. (2010). "Finite-element modeling of nonlinear behavior of masonry-infilled RC frames." *J. Struct. Eng.,* 136(3), 285-296.

[9] Mosalam, K. Gunay S. and Sweat, H. (2013). "Simulation of reinforced concrete frame with unreinforced masonry infilled walls with emphasis on critical modeling aspects." *Proc., 12th Canadian Masonry Symposium*, Vancouver, BC, Canada.

[10] ATC-24, (1994). *Guidelines for cyclic seismic testing of components of steel structures*, Applied Technology Council, Redwood City, CA.

[11] Mazzoni, S., McKenna, F., Scott, M. H. and Fenves, G. L. and others. (2006). "*OpenSees command language manual*," Pacific Earthquake Engineering Research (PEER) Center, Berkeley, CA.

[12] El-Dakhakhni, W., Elgaaly, M. and Hamid, A. A. (2003). "Three-strut model for concrete masonry-infilled steel frames," *J. Struct. Eng.,* 129(2), 177-185.

[13] Dolsek, M. and Fajfar, P. (2008). "The effect of masonry infills on the seismic response of a four-storey reinforced concrete frame — a deterministic assessment." *J. Struct. Eng.,* 30(7), 1991–2001.

[14] Filippou, F. C., Popov, E. P. and Bertero, V. V. (1983). "Effects of bond deterioration on hysteretic behavior of reinforced concrete joints." *(Report NO. UCB/EERC-83/19), Pacific Earthquake Engineering Research center (PEER)*, Berkeley, CA.

[15] Monti, G. and Spacone, E. (2000). "Reinforced concrete fiber beam element with bond-slip." *J. Struct. Eng.,* 126(6), 654-661.

[16] Mander, J. B., Priestley, M. J. N. and Park, R. (1988). "Theoretical stress-strain model for confined concrete." *J. Struct. Eng.,* 114(8), 1804-1825.

[17] Karsan, I. D. and Jirsa, J. O. (1969). "Behavior of concrete under compressive loading." *J. Struct. Eng.,* ST12(95).

[18] Dvorkin, E. N., Pantuso, D. and Repetto, E. (1995). "A formulation of the MITC4 shell element for finite strain elasto-plastic analysis." J. *Meth. in Appl. Mech. and Eng.,* 125(1), 17-40.

[19] Lu, X. Lu, X. Z., Guan, H. and Ye, L. P. (2013). "Collapse simulation of reinforced concrete high–rise building induced by extreme earthquakes." *J. Earth. Eng. Struct. Dyn.,* 42, 705-723.